Radar Observations of Winds and Turbulence in the Stratosphere and Mesosphere

RONALD F. WOODMAN AND ALBERTO GUILLEN

Radio Observatorio de Jicamarca, Instituto Geofísico del Perú, Lima

(Manuscript received 16 August 1972, in revised form 19 September 1973)

ABSTRACT

A technique for the observation of radar echoes from stratospheric and mesospheric heights has been developed at the Jicamarca Radio Observatory. Signals are detected at the altitude ranges between 10–35 km and from 55–85 km with powers from many to several tens of decibels above noise level. The three most important frequency spectrum characteristics—power, Doppler shift and spectrum width—are observed in real time. The power levels as well as the spectral width are explained in terms of turbulent layers, with a thickness of the order of 100 m, in regions with a positive potential temperature or electron density vertical gradients. Continuous wind velocity records are obtained with a precision of the order of 0.02–0.2 m sec^{-1} for the vertical component and 0.20–2 m sec^{-1} for the horizontal, with a time resolution of the order of 1 min. The highest precisions are obtained at stratospheric heights. Fluctuations in velocity in the mesosphere are observed at the shortest gravity wave periods with amplitudes of the order of 1 m sec^{-1} for the vertical component and of 10 m sec^{-1} for the horizontal. Tidal components at these altitudes are not as large as predicted by theory. A technique to obtain the power, the Doppler shift, and the width of the frequency spectrum of the echo signals from only two points of the correlation function is described.

1. Introduction

Radar techniques have proved to be a very powerful tool for the study of the earth's upper and lower atmosphere. There are two relatively unconnected groups using powerful radars to study the earth's atmosphere. One of them, using the scattering properties of free electrons, has been studying the earth's ionosphere, the other, using the scattering property of water or ice particles and/or the fluctuations of index of refraction in clear air, has been dedicated to the study of meteorological phenomena in the troposphere.

Most of the work of the first group has been confined, either by interest or system capabilities, to the region between 90 and 10,000 km altitude, with special emphasis in the 200–700 km range [see Evans (1969) for a review]. The technique used is known in the literature as the "incoherent scatter" or "Thomson scatter" technique. Most of the important parameters that define the earth's ionosphere have been measured and studied this way. Several powerful radars have been designed and built for this purpose, among them the Jicamarca radar (11.95°S, 76.87°W) located near Lima, Peru, with which we are concerned in this paper.

The meteorological group has mainly limited its observations and studies to altitudes up to 10–12 km. Radar techniques have been used as powerful research tools to study clear air turbulence, cloud physics, and dynamics of convective storms and large-scale storms [see Wilson and Miller (1972) and Hardy (1972) for a review].

Very little work has been done by either group in the height range between 15 to 85 km. The authors are aware of only one effort to obtain radar echoes from stratospheric heights (Crane, 1970). Although a very powerful radar was used, the echo signals received were barely above the sensitivity of the system.

The purpose of this paper is to report observations made with the Jicamarca radar within the 15–85 km range. We also describe the techniques developed for this purpose. As we shall see in more detail the echoes obtained from this region come from backscattering produced by dielectric constant fluctuations of the medium with scale sizes of the order of 3 m. Analysis of these signals yields information about the dynamics of large-scale phenomena, using the 3 m fluctuations as tracers of their motions, as well as information on the degree of turbulence at a 3 m wavelength.

We have obtained usable echoes from two well-defined regions: one at stratospheric heights between 15 to 35 km, and the other at mesospheric heights from 60 to 85 km. The latter corresponds to the D region of the ionosphere. The echoes, after digital filtering, are from several decibels to several tens of decibels above the noise level.

The dielectric properties and, therefore, the dielectric fluctuations within these two regions, are produced by different physical phenomena. In the stratosphere, the dielectric properties are determined by the density of the atmosphere (i.e., by its temperature at a given pressure), and in the D region by the number of free electrons. Nevertheless, we are reporting our observations of both regions together since they are observed with exactly the same techniques and, as far as the interpretation of larger scale phenomena (winds, gravity waves, etc.), the dielectric fluctuations are used as simple tracers; the results are independent of the mechanisms responsible for the fluctuations.

First, we shall review some important conclusions from electromagnetic wave scattering theory and then briefly describe the Jicamarca radar, including some important parameters used. We follow with a description of the observing techniques and discuss at some length the data processing. We have used unconventional processing methods which we believe should benefit readers concerned with meteorological and incoherent scatter radars because of their simplicity and time-saving advantages. We then proceed to discuss some preliminary results as well as the full potential of the radar.

2. Backscattering theory

If a dielectric medium is illuminated by an electromagnetic wave, the wave propagates according to the refractive and attenuating properties of the medium. If the medium is "transparent," most of the signal power goes through but for the fraction of the electromagnetic energy which is partially reflected at the interfaces or converted to a different kind of energy (attenuation). In addition, in any dielectric, no matter how transparent, a fraction of the power carried in the primary wave is scattered in all directions. The scattering can be traced to the oscillations induced to the electrons, either bound or free, which are constituents of the medium. The average density of the oscillating electrons is responsible for the average dielectric properties of the medium and the density fluctuations for the scattering. The density fluctuations are always present because of the discrete nature of the electrons, or of the molecules and atoms of which they are a part.

Fluctuations in a medium are a random process in space and time, and are characterized statistically by its space-time autocorrelation function. If $n(\mathbf{x},t)$ is the fluctuating index of refraction of the medium at a point $\mathbf{x}$ in space and t in time, then the space-time autocorrelation function, $\rho(\mathbf{r},\tau)$ is defined by the average

$$\rho(\mathbf{r},\tau)=\langle n(\mathbf{x},t)n(\mathbf{x}+\mathbf{r},\, t+\tau)\rangle-\langle n(\mathbf{x},t)\rangle^2. \quad (1)$$

If this medium is illuminated with an electromagnetic wave, it can be shown that the amplitude of the linearly detected scattered wave, $E_s(t)$, is a Gaussian random process and its time correlation function $C(\tau)=\langle E_s(t)E_s^*(t+\tau)\rangle$ is given by

$$C(\tau)=Kk^4\hat{\rho}(\mathbf{k},\tau), \quad (2)$$

and its frequency spectrum $F(\omega)$ by the time Fourier transform of $C(\tau)$. Here K is a proportionality constant which depends on the geometry of the antennas and transmitter characteristics, and $\hat{\rho}(\mathbf{k},\tau)$ is the space Fourier transform of $\rho(\mathbf{r},\tau)$ evaluated at $\mathbf{k}=\mathbf{k}_i-\mathbf{k}_s$, i.e.,

$$\hat{\rho}(\mathbf{k},\tau)=\frac{1}{8\pi^3}\int d\mathbf{r}\exp(-j\mathbf{r}\cdot\boldsymbol{\xi})\rho(\mathbf{r},\tau)\bigg|_{\xi=\mathbf{k}}, \quad (3)$$

where $\mathbf{k}_i$ and $\mathbf{k}_s$ are the wave vectors of the incident and scattered wave, respectively.

The dependence expressed in Eq. (2) of the statistical properties of the scattered signal, represented by $C(\tau)$, on $\hat{\rho}(\mathbf{k},\tau)$, tell us that, if we are to consider the fluctuations in the dielectric medium as the Fourier superposition of waves with all vector numbers $\boldsymbol{\xi}$, then only the wave component with wavenumber $\mathbf{k}=\mathbf{k}_i-\mathbf{k}_s$ contributes to the scattering. Furthermore, it tells us that the statistical-dynamical properties of the signal received are directly related to the dynamics of this component ($\mathbf{k}$).

For the case of backscattering, $\mathbf{k}_i=-\mathbf{k}_s$ and $\mathbf{k}=2\mathbf{k}_i$; therefore, only wave fluctuations in the direction of the illuminating wave and with a wavelength equal to half the wavelength of the electromagnetic wave (3 m for the Jicamarca radar) contribute to the backscattering.

The fluctuations in dielectric constant responsible for the scattering are at a minimum level when the medium is homogeneous and in thermodynamic equilibrium, but they can be enhanced to very large amplitudes either by external means or by intrinsic unstable processes. When the scattering is produced by fluctuations at the thermal level we will refer to it as "thermal scattering" or "incoherent scattering." If the scattering is produced by enhanced fluctuations we will refer to it as "non-thermal scattering." We should note that incoherent scattering is not a a very proper name since non-thermal scattering is also incoherent, unless the enhanced fluctuations are of deterministic nature or there is statistical coherence (correlation) between them and the phase of the primary wave. We use the term incoherent in any case, since it has been extensively used in the literature in this restrictive sense.

The success of the incoherent scatter technique in the field of ionospheric physics relies mainly on the fact that the electron gas in the ionosphere is in thermodynamic equilibrium; suitable theories have been developed to predict the dependence for the statistical properties of the scattering signal, namely $C(\tau)$ [or its transform, the frequency spectrum $F(\omega)$], on the thermodynamic parameters that define the medium. In contrast, the echoes received from the stratospheric and mesospheric heights, that concern us in this paper, are so enhanced over thermal scattering that one cannot assume, as it is done for the ionosphere, that the medium is in thermal equilibrium. The statistical properties of the signals received, therefore, do not contain as much information as those of signals obtained from ionospheric heights. Nevertheless, the sta-

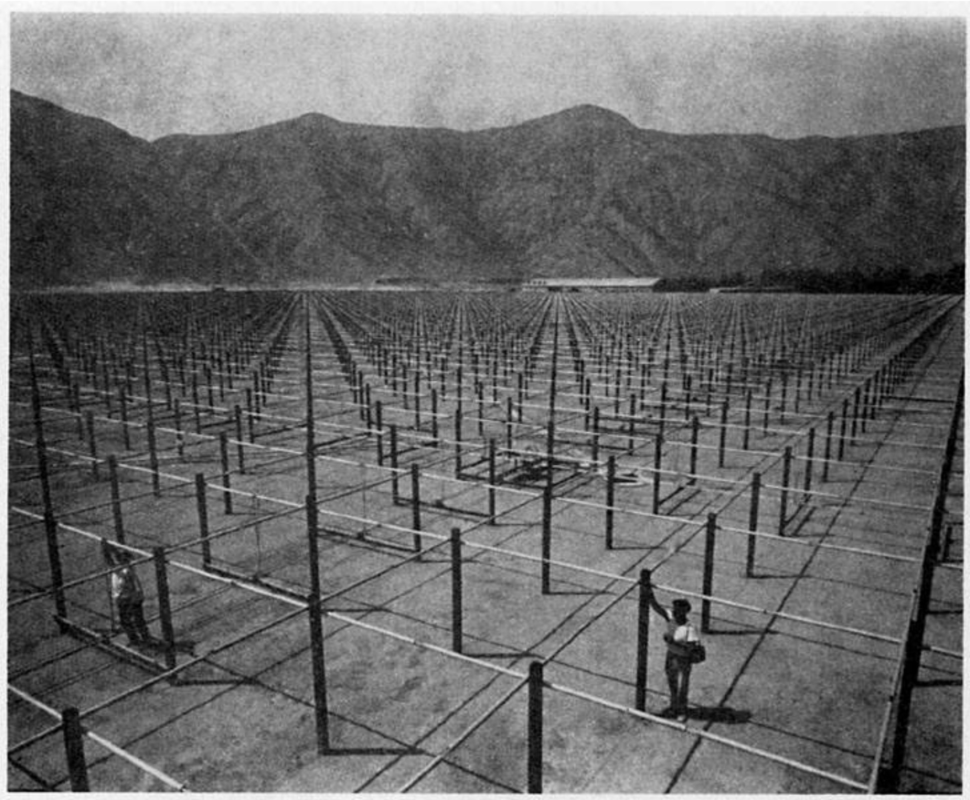

FIG. 1. A view of the Jicamarca Radio Observatory. The antenna consists of 9216 crossed dipoles in a square array 300 m along a side.

tistical properties of these signals still carry important information about these regions of the atmosphere, information that has not been obtained using other techniques.

There are three statistical parameters of interest which will be discussed in this paper: the power, the Doppler shift, and the width of the frequency power spectrum of the scattered signals received. They correspond to the three first moments of the frequency spectrum, and are related to the fluctuation intensity (degree of turbulence), the velocity of the medium in the scattering volume, and the distribution of random velocities within the scattering volume, respectively.

3. Equipment description

As mentioned earlier, the Jicamarca radar was specially designed and built to study the ionosphere using incoherent scatter techniques. It operates at 50 MHz, has an antenna with a collecting area of 8.4×10^4 m^2, the largest in the world (see Fig. 1). It consists of two superimposed square arrays of 9216 half-wave (3 m) dipoles, one for each linear orthogonal polarization. The dipoles of each polarization are interconnected in phase to form 64 square modules. The modules in turn are grouped into four squares with four independent feeds. The pointing direction of each module is fixed. They point to the zenith of the observatory (1.50° southeast of the observatory, to be exact). By properly phasing each of the 64 modules, it is possible to tilt the direction of the full antenna, approximately 3° from zenith, limited by the beamwidth of each module. Different polarizations, or different quarters of the antenna, can be adjusted to point to different directions simultaneously. The beamwidth of the full antenna is 1° to the half-power point, giving an effective width of 0.7° when working as a radar.

The transmitter system consists of four independent transmitter units of 1 MW peak power each, at a maximum 6% duty cycle. They can be driven in phase and have provisions for parallel operation into a single load.

The same antenna is used for reception in a radar fashion. The backscatter signals are coherently detected after amplification in appropriate receivers. The detected signals are digitalized and statistically analyzed in a special programmable correlator tied to a general purpose computer. For the particular application described in this paper, the correlator was programmed to work as a digital filter and the statistical processing was performed in a general purpose computer. This computer is an old and very slow machine according to modern standards, limiting observations to only one height at a time, even though we have used some efficient processing techniques as described in the data processing section. These same techniques will allow us to process in real time all observable heights simultaneously when a third-generation computer already available in the Observatory is connected to the system.

All the observations reported here have been obtained using 1 MW peak power with a pulse width of 33 μsec and a receiver bandwidth of 30 kHz, giving a system height resolution of the order of 5 km. A pulse repetition rate of $\sim$700 μsec has been used.

4. Observational techniques and data processing

The coherently detected amplitude $E(t)$, corresponding to the backscattered signal from a given height, forms a discrete complex Gaussian random process in time with sample points for each radar pulse transmitted at times $t=t_1, t_2 \ldots t_j \ldots t_n$. It is fully characterized statistically by its time autocorrelation function $C(\tau)=\langle E(t)E^*(t+\tau)\rangle$, or by the Fourier transform $F(\omega)$, of $C(\tau)$. We have seen in Section 2 that they are directly related [by Eq. (2)] with $\hat{\rho}(\mathbf{k},\tau)$, which in turn fully characterizes the time behavior of the 3 m wave component of the fluctuations in index of refraction in the medium.

Of all the information contained in either member of the transform pair, one is specially interested, as in many other physical processes, in three particular parameters; the power P of the signal, the mean frequency shift Ω, and the width σ of the frequency spectrum. They are directly related to the three first moments of the frequency spectrum m_0, m_1, m_2, as follows:

$$P=m_0, \tag{4}$$

$$\Omega=m_1/m_0, \tag{5}$$

$$\sigma^2=\frac{m_2}{m_0}-\left(\frac{m_1}{m_0}\right)^2, \tag{6}$$

where

$$m_0\equiv\int F(\omega)d\omega, \tag{7}$$

$$m_1\equiv\int \omega F(\omega)d\omega, \tag{8}$$

$$m_2\equiv\int \omega^2 F(\omega)d\omega. \tag{9}$$

The importance of these three parameters rests in the fact that they are directly related with three important properties of the scattering medium.

The power P is directly proportional to $\phi(k)\equiv\hat{\rho}(\mathbf{k},0)$, which evaluates the spatial spectrum of the fluctuations at a given wavenumber k (3 m in our case). If the shape $\phi(\xi)$ of the spectrum is known, it gives information about the mean square of fluctuations in index of refraction, $\langle(n-\langle n\rangle)^2\rangle$.

The mean frequency shift is the Doppler shift produced by the mean velocity v of the scattering volume. It is related to the latter by $v=\Omega c/(2\omega_0)$, where ω_0 is the transmitter frequency.

The spectrum width is related to the root mean square of velocity fluctuations from the mean, or to the diffusion velocity (life-time) of structure in the 3 m scale, whichever is faster.

There is no need to stress the importance of the three mentioned parameters in the turbulent processes of the atmosphere, and we shall return to them when we discuss our observations.

We can considerably simplify the data processing if we limit ourselves to the three mentioned moments of the frequency spectrum, since this information can be obtained from a single point evaluation at the origin ($\tau=0$), of the correlation function $C(\tau)$ and its first and second derivative, $C'(\tau)$ and $C''(\tau)$. This follows from the fact that the frequency spectrum and the autocorrelation function are Fourier transforms of each other, and it is known that the moments of one are related to the derivatives of the other evaluated at the origin. Specifically, we have the well-known relationship

$$P=C(0), \tag{10}$$

and it can be shown that (see Appendix A)

$$\Omega=\phi'(0), \tag{11}$$

$$\sigma^2=\frac{A''(0)}{C(0)}. \tag{12}$$

Here $\phi'(0)$ and $A''(0)$ are the first derivative of the phase, $\phi(\tau)$, and the second derivative of the absolute value, $A(\tau)$, of the correlation function evaluated at $\tau=0$, respectively. If we take a time delay τ_1 sufficiently small for high-order terms of a Taylor expansion of $\phi(\tau)$ and $A(\tau)$ to be negligible, we can write (see Appendix A)

$$\Omega=\frac{\phi(\tau_1)}{\tau_1}, \tag{13}$$

$$\sigma^2=2\frac{1-A(\tau_1)/C(0)}{\tau_1^2}. \tag{14}$$

Eqs. (10), (13) and (14) imply that we can evaluate P, Ω and σ^2 from only two points of the complex correlation function, one at the origin and the other at a convenient delay τ_1. This involves the estimation of the average of only two products, $\langle|E^2(t)|\rangle$ and $\langle E(t)E^*(t+\tau_1)\rangle$, a considerable simpler and faster operation compared with a complete estimation of the frequency spectrum of the process.

It should be pointed out that if the spectrum is symmetric (i.e., if random velocities are equally likely above and below the mean) Eq. (13) becomes an identity (see Appendix A), and that many frequency spectrum functions, including Gaussian, are completely defined if the three first moments are known.

The statistical errors of the estimates of σ and Ω using Eqs. (13) and (14) are comparable to the ones obtained through a full spectrum integration. This should not be unexpected since it is simply an extension of the technique of evaluating the power by estimating $C(0)=\langle E^2(t)\rangle$ rather than from $\int F(\omega)d\omega$. The statistical error $\Delta\Omega$ in the estimate of Ω is given by Woodman and Hagfors (1969) as

$$\langle\Delta\Omega^2\rangle=\frac{1-S^2}{2NS}, \tag{15}$$

where N is the number of sample points averaged and S the normalized autocorrelation at τ, normalized with respect to total power including receiver and sky noise.

As we shall see later when we present the results, the correlation time of the backscatter signals is very long, of the order of 1 sec, i.e., much longer than the 700-μsec inter-pulse period. This has permitted us to improve the signal-to-noise ratio by coherently averaging many transmitter pulses together. The results reported here have been obtained by averaging 316 pulses to make a sample point, giving a signal-to-noise improvement of 25 dB over the ratio obtained from a single radar pulse. This improvement results from the fact that the signal, being coherent, adds to an amplitude ~316 larger, whereas the noise which is incoherent from pulse to pulse, adds as the square root of 316.

This integration scheme also reduces considerably the statistical processing time, by reducing the number of sample points.

The summation of 316 pulses gives a pre-detection integration time of 0.22 sec which should not be confused with the post-detection integration time used to obtain the estimates of the different quadratic statistical averages. We have used 1 or 2 min for the latter, which determines the time resolution in the continuous measurement of any of the parameters (power, velocity and width) mentioned earlier.

The second integration time also determines the uncertainty in the parameter measured, given a signal-to-noise ratio (much larger than 1 for most of the times and height ranges reported) and a correlation width. Typical uncertainties are of the order of 10% for the power measurements, one to a few cm sec^{-1} for the velocity measurements at stratospheric heights, and ten to a few tens of cm sec^{-1} at mesospheric heights.

The radar gives us only the projection of the velocity of the scattering medium along the direction of propagation of the probing wave. The projection in the transverse direction can be obtained by pointing simultaneously at two different directions, provided that the scale size of the velocity field of the medium is much larger than the separation between the two scattering volumes defined by the two pointing directions. This has been done with the Jicamarca antenna by pointing one of the polarizations in a given direction as far from

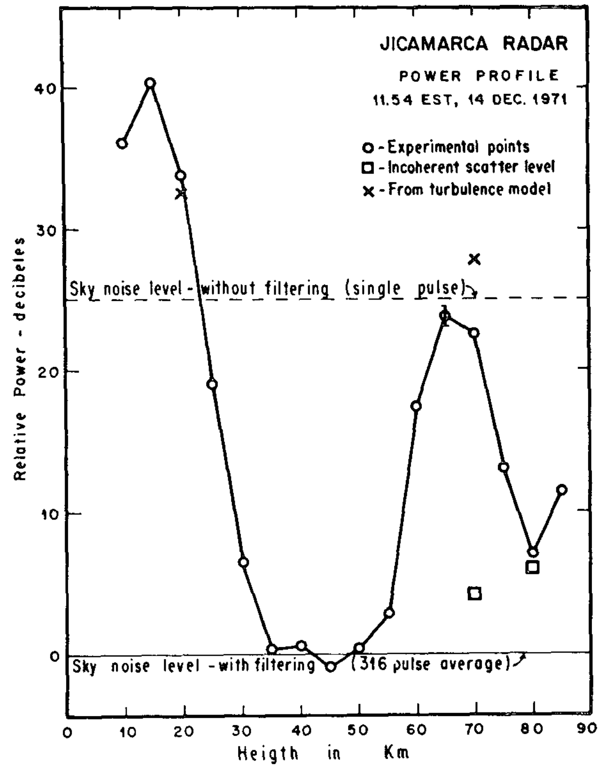

FIG. 2. Backscatter power profile obtained from fluctuations in index of refraction in the upper atmosphere with the 50-MHz Jicamarca radar. The incoherent scatter levels correspond to 0.5×10^9 and 10^9 electrons m^{-3} at 70 and 80 km, respectively. The turbulence models assume $L_0=100$ m.

the zenith as possible and the other polarization away from the zenith in an opposite direction. Having the projections in two different directions, the projections in any other two directions within the same plane can be obtained by simple linear transformations. The vertical and E–W horizontal projections of the winds have been obtained by pointing the two antennas at approximately 3° west and east of the zenith. The vertical and N–S components have been obtained by a similar split in the north–south direction.

With a 6° split in an almost vertical configuration, the vertical velocities are obtained with the same accuracy as the figures mentioned before. The accuracy for the horizontal projection is deteriorated by a factor of order 10 [from $(\sin 6°)^{-1}=10$], which still gives acceptable values of the order of 20 cm sec^{-1} for the stratosphere and 2 m sec^{-1} for the mesosphere.

The resulting separation of the scattering volumes are of the order of 3–10 km which is smaller than the wavelength of gravity waves and certainly smaller than the scale size of winds of longer duration.

Because of computer speed limitations only one height can be observed at a time. A system using a third-generation computer is being implemented which should permit us to observe about 20 heights simultaneously.

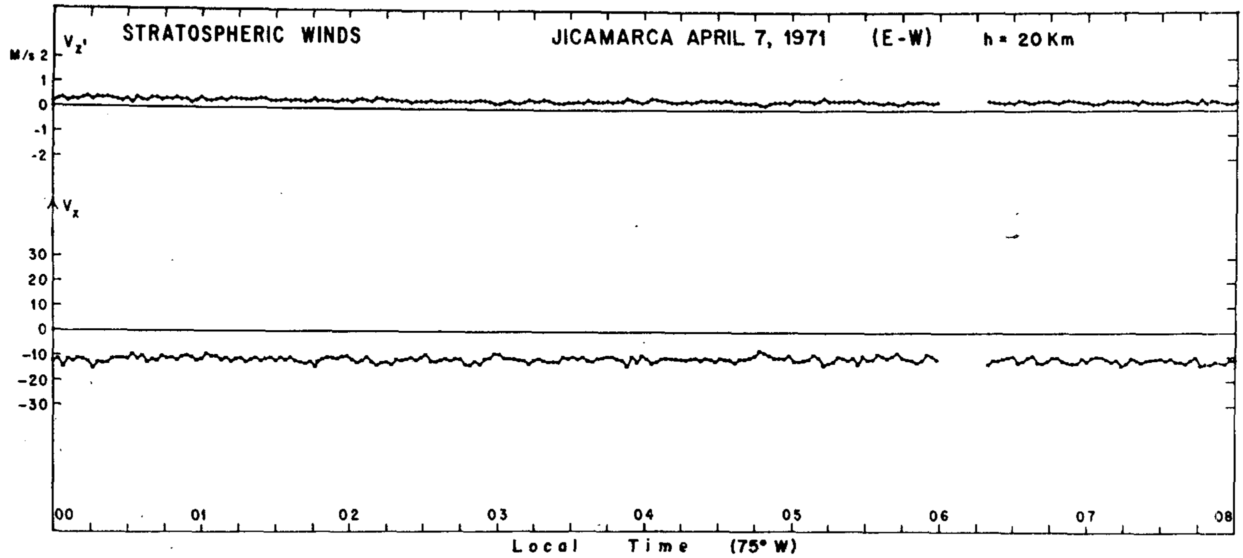

FIG. 3. Record of easterly (V_x) and vertical velocities (V_z) at 20 km obtained from the Doppler shift of radar backscatter echoes.

5. Results

a. Power measurements

Fig. 2 shows a profile of the echo power, $\langle E(t)^2 \rangle$, in decibels, as a function of height obtained with the Jicamarca radar. The noise level is shown as a reference level. In our receiver installation the noise is mainly of cosmic origin, corresponding to a sky temperature of approximately 5000K. The peak transmitter power was 1 MW with pulses 5 km wide and an i.f. receiver bandwidth of 30 kHz. The noise level in the hypothetical case that no coherent integration had been used is shown with a dotted line. The different heights were observed sequentially with 2 min integration for each.

It is interesting to compare the echo with what one would receive from pure thermal scattering. A thermal plasma at 80 km with a free density of 10^3 electrons cm^{-3} would produce an echo (using the same averaging technique) at the 7-dB level. This level is also shown in Fig. 2.

From Fig. 2 it is apparent that there are two regions of enhanced fluctuations detectable with the existing system sensitivity, one at stratospheric heights up to 30 km, the other from 55–85 km (sometimes merging into the E region). The power level at 80 km is of the order of the incoherent scatter level for this particular run, but this is not the usual case. One hour before, this level was an order of magnitude higher. On occasions, power levels above the noise level are observed at the 35-km level.

It is not possible to make good observations below about 15 km because of ground clutter from the nearby mountains (the 10-km value should be taken with caution). Although there is also some weak ground clutter at other heights, this has been filtered out by taking advantage of its Doppler frequency characteristics; coherent detection is used and since fixed targets produce a spectral line at the transmitter frequency, it can be notched out digitally provided the clutter-to-signal ratio does not exceed the dynamic range of the instrument.

There are enhanced echoes beyond 85 km but they will not be discussed here. In this region the electrons have sufficient mobility to be affected by the existing electric fields and deserve a different treatment. This height range corresponds to the electrojet region, which has been extensively discussed elsewhere (Balsley, 1969; Farley, 1963).

Continuous records of power as a function of time at one particular height have also been obtained. The echoes from stratospheric heights (15–35 km) are relatively constant in amplitude. They persist throughout 24 hr of the day and show little variation from day to day. The echoes from mesospheric heights (55–85 km), on the other hand, are quite variable. They are absent during nighttime hours and vary considerably during the day, and from one day to the other. They commonly present a feature which is not apparent in Fig. 2—the existence of well-defined layers narrower than the present resolution of our system (5 km). These layers produce echoes much larger than the ones obtained from neighboring heights and persist for several hours at one or two preferred heights. These echoes appear at times 10–15 dB stronger than the background level even before any digital integration has taken place. They appear clearly on an oscilloscope display of the radar receiver. The existence of these layers has been reported and discussed previously by Flock and Balsley (1967). Typical daily records have been reported by Rastogi and Woodman (1974).

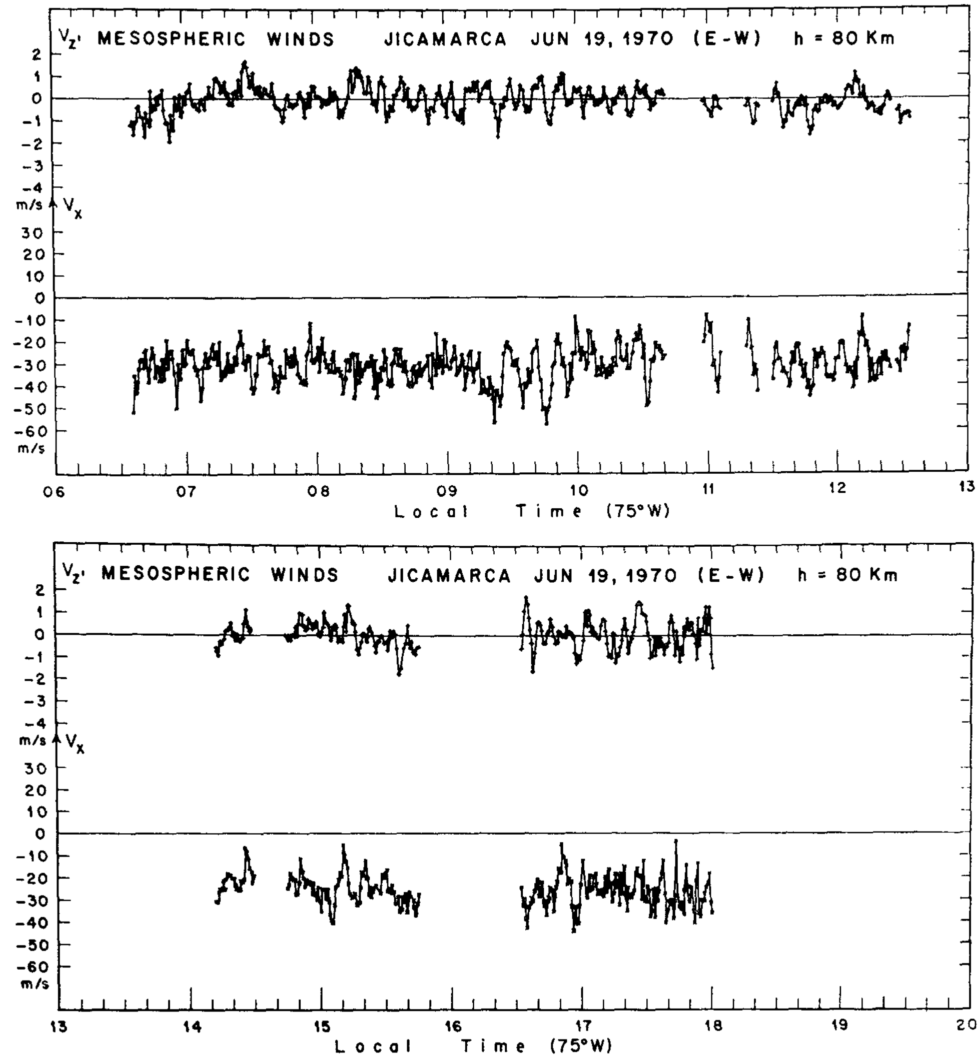

FIG. 4. Two records of easterly and vertical velocities at 80 km obtained from the Doppler shift of radar backscatter echoes.

b. *Wind measurements*

Fig. 3 shows a record of stratospheric velocities as a function of time obtained using the above-mentioned technique. Points are taken with a 2-min integration time. The data were taken looking east and west from the vertical and have been processed to show the east–west and vertical components. The accuracy of the technique is evident from the record. Note that the vertical and horizontal velocity scales differ by a factor of 10. Most of the fluctuations are real since they are larger than the expected uncertainty and correlate from point to point (noise deviations are statistically independent for adjacent points). The small bias on the vertical component is due to some contamination from the N–S projection of the wind. The geometrical axis of the antenna is tilted 1.04° to the south and the two pointing directions of the antenna were not on an exactly vertical plane.

Several days of data taken at this or other stratospheric heights all show similar features. The mean velocity is relatively constant as a function of time of day with very small fluctuations of the order of 2 m sec^{-1} for the horizontal and 10 cm sec^{-1} for the vertical. The amplitude of the fluctuations is larger for greater heights.

Figs. 4a and 4b show the same type of data but for 80 km in the mesospheric region. In this case the fluctuations are much larger, of the order of 10 m sec^{-1} for the horizontal and 1 m sec^{-1} for the vertical. The time resolution is 1 min, clearly defining oscillations with periods as short as ~5 min. The potential of the technique for the study of gravity waves including periods close to the Brunt-Väisälä cutoff frequency is evident.

Similar data have been obtained on different days with a N–S antenna split to obtain the N–S velocity

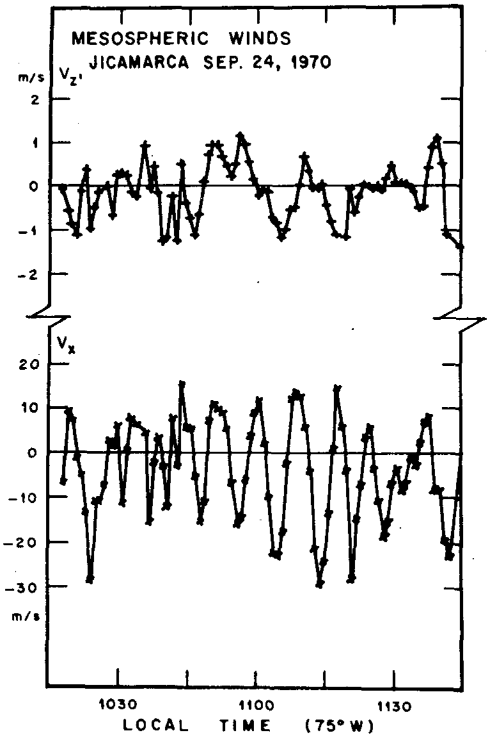

FIG. 5. Sample record of velocities at 85 km showing large sinusoidal fluctuations with gravity wave periods.

component. On occasions, well-defined quasi-sinusoidal oscillations are observed. A selected sample is shown in Fig. 5.

Observations at mesospheric heights are limited to daytime hours when there is sufficient backscatter power. The mean zonal and meridional velocities are of the order of a few tens of meters per second, the meridional velocities being smaller. As shown in Fig. 4 for this particular height and for the latitude (−12S) of the Jicamarca Observatory, there is no evidence of diurnal or semidiurnal components with magnitudes as large as the 30 m sec^{-1} predicted by theory (Lindzen and Chapman, 1969).

c. *Spectrum width measurements*

Typical frequency power spectrum widths σ are shown in Fig. 6. They correspond to the power profile shown in Fig. 2. In the same figure the half-correlation width $\tau_{\frac{1}{2}}$ is shown, defined as the inverse of the spectrum width, $1/\sigma$. This second parameter can also be interpreted as the delay at which the parabola defined by the truncated Taylor series has a value equal to half the maximum correlation at zero delay. Typical values of the order of 2 sec for stratospheric heights and of 1 sec for mesospheric heights clearly justify the coherent integration times of the order of $\frac{1}{4}$ sec which have been used for the processing of the signals.

6. Discussion

a. *Power and spectrum width*

As mentioned in the Introduction, we are postulating that clear air turbulence is the mechanism responsible for the enhancement of the dielectric fluctuations in the stratosphere, which, in turn, are responsible for the strong radar echoes received from these height ranges. Turbulence in a region with a negative lapse rate, as in the stratosphere, is very efficient in producing fluctuations in temperature and hence in index of refraction. If a parcel of air is transported up, adiabatically, in a region where a negative lapse rate exists, it will cool at the same time it moves into a higher temperature region; similarly, a parcel of air that moves down will become warmer as it moves into a cooler background, hence producing fluctuations in temperature. This is the same mechanism postulated by Booker and Gordon (1957) to explain forward stratospheric scattering of UHF and VHF frequencies.

In what follows we shall make theoretical computations to show that such a mechanism is indeed possible. Furthermore, we shall conclude that the turbulent region must be confined to one or a few layers close to 100 m in thickness to explain the power levels received as well as the width of the frequency spectrum.

We need to recall the following relationships taken from Tatarski (1961). In the inertial subrange (to be justified *a posteriori*)

$$\phi_n(k)=0.033C_n^2k^{-11/3}, \tag{16}$$

where $\phi_n(k)$ is the three-dimensional space spectrum of the fluctuations in index of refraction, corresponding to $\hat{\rho}(k,0)$ in our notation in Eq. (2); k is the wavenumber ($=2.09$ m^{-1}); and C_n^2 an amplitude factor given by

$$C_n=aL_0^{4/3}\left(\frac{dN}{dz}\right). \tag{17}$$

Here a is a proportionality constant of order unity, L_0 the largest scale size of eddies, and dN/dz the gradient in potential index of refraction given by

$$\frac{dN}{dz}=\frac{-79\times10^{-6}p}{T^2}\left[\left(\frac{dT}{dz}\right)+\gamma_a\right], \tag{18}$$

where p is the pressure (mb), T the temperature of the medium (°K) and γ_a the adiabatic lapse rate (°K m^{-1}).

The only parameter at our disposition is L_0. We shall initially assume for our discussion $L_0=100$ m corresponding to a turbulent layer of equivalent thickness.

For the above listed parameters the resultant value of $\phi(k)$ is

$$\phi'(k)=6.8\times10^{-19}\text{ m}^3. \tag{19}$$

With this value and the radar parameters we should be in position to calculate the expected backscattered power. To avoid using the radar equation and un-

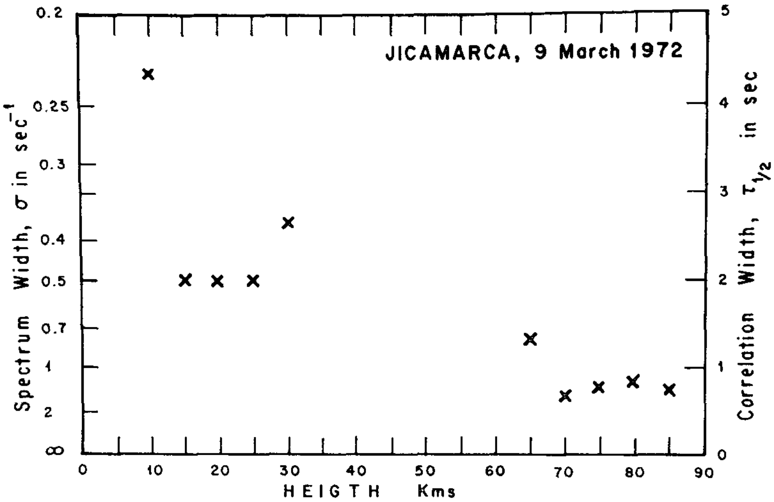

FIG. 6. Typical spectrum width of the backscatter echoes. The right-hand scale gives the correlation width.

calibrated radar parameters, we have used radar echoes from ionosphereric heights as a calibrating signal. If we use the same radar parameters for both heights, we have

$$P=\frac{\phi_n(k)}{\phi_n'(k)}\frac{R'^2}{R^2}\frac{L}{L'}P', \tag{20}$$

where P is the signal power, R the distance to the scattering volume, and L the depth of the scattering volume. The primes denote the same variables for ionospheric heights. We shall use $R=20$ km, $R'=400$ km, $L'=5$ km (the pulse length), and $L=L_0=100$ m. The value of $\phi'(k)$ can be calculated very accurately from incoherent scatter theory. In Appendix B we have derived an expression of the form

$$\phi'(k)=\frac{1}{8\times(2\pi)^3}\frac{f_p^4}{f^4N}, \tag{21}$$

where N is the number of electrons per cubic meter, f_p the corresponding plasma frequency, and f the frequency of the probing wave (50 MHz). For an electron density of 2×10^{12} electrons m^{-3}, f_p is 12.5×10^6 MHz, and

$$\phi'(k)=9.8\times10^{-19}. \tag{22}$$

The same ionospheric and radar parameters give an experimentally obtained signal of 0 dB above the noise level. Using this value in Eq. (20) for the calibrating power, we predict a non-filtered signal of 7.5 dB above the noise level for the model at 20 km altitude. This value is also shown in Fig. 2 and is very close to the measured power at this altitude. We conclude then that our model with a turbulent layer of 100 m is consistent with the power measurements.

Note that we have used the noise level without filtering, corresponding to a system without the coherent integration scheme, since no such integration can be performed at the ionospheric heights used for calibration. The coherence time at these altitudes is of the order of 1 msec.

The postulated mechanism as well as the layer thickness should also agree with the frequency spectrum width. The spectrum shape can be related to the random velocity of independently scattering elements, each contributing with its own Doppler shift. The spectrum width σ would then be the variance, $\langle(\omega-\Omega)^2\rangle^{\frac{1}{2}}$, of the Doppler shift deviations of each contributing element, and should be proportional to the variance of the random velocity fluctuations, $u=\langle\Delta v^2\rangle^{\frac{1}{2}}$; that is, σ can be related to u by

$$\sigma=\frac{2u\omega_0}{c}, \tag{23}$$

where c is the speed of light and ω_0 the radar frequency. For a measured value 0.5 sec^{-1} of σ, and the frequency used, σ corresponds to an rms velocity u of 0.25 m sec^{-1}.

The value of u depends, according to turbulence theory, on the velocity shear and the thickness of the sheared region which has become turbulent. According to Tennekes and Lumley (1972) it is of the order of $\frac{1}{6}$ of the difference in the mean velocities within the unstable shear region.

We shall assume that the sheared region has just gone critical, i.e., it has just met the Richardson energy criterion. It is difficult to sustain higher velocity gradients since turbulence greatly enhances the effective viscosity. The Richardson energy criterion is met whenever

$$\mathrm{Ri}=\frac{d}{dz}(\ln\Theta)\Big/\left(\frac{du}{dz}\right)^2\leqslant0.25, \tag{24}$$

where g is the gravitational acceleration, and Θ the potential temperature.

At an altitude of 20 km and in an isothermal atmosphere, Ri = 0.25 when $du/dz = 4\times10^{-2}$. This is also about the maximum value observed (Barbé, 1971; Cadet, 1973) by *in-situ* measurements. To this value of velocity gradient the maximum difference of mean velocities in a 100 m layer is 4 m sec^{-1}. Applying the $\frac{1}{6}$ factor mentioned earlier, we get an estimated value of u of the order of 0.6 m sec^{-1}, which is of the same order of magnitude as the value estimated from the spectrum width (0.25 m sec^{-1}).

If we postulate a turbulent layer of 40 m we would get perfect agreement for the spectrum width but the resultant power would become smaller. The agreement with both measurements can be improved by assuming more than one layer within the 5-km region defined by the pulse length. The power level at 30 km can be explained in a similar way with no more than one layer of 40 m in thickness. Given the crudeness of turbulence theory, implicit in the value of the constant a and in the definition of the scale size L_0, we should consider the agreement as satisfactory and conclude that one or a few clear air turbulent layers with a thickness of the order of 40–100 m will explain the power levels and spectrum width characteristics of the echoes received from stratospheric heights.

We have assumed in Eq. (16) that a wavelength of 3 m falls within the intertial subrange. Eq. (16) is valid provided that $\lambda = 2\pi k^{-1}$ is within l and L_0, i.e., $l > \lambda < L_0$, where

$$l = \frac{L_0}{\mathrm{Re}^{3/4}}, \tag{25}$$

where Re is the Reynolds number. For the given parameters, $l = 0.5$ cm, so the use of Eq. (16) is well justified.

As it has been mentioned before, Crane (1970), using a powerful L-band radar at Millstone Hill, Mass., has obtained stratospheric echoes from 20-km altitudes with strengths barely above the sensitivity of the radar. The signal strengths correspond to a value of $C_n^2 = 10^{-16}$ m$^{-\frac{2}{3}}$, if one assumes that the turbulent layer is homogeneous and fills the volume defined by the radar pulse length (1.1 km), or, to $\sim 10^{-15}$ m$^{-\frac{2}{3}}$ if the layer is only 100 m thick. At Jicamarca the corresponding value of C_n^2 is 0.35×10^{-15}, i.e., in very good agreement with Crane's results considering the assumptions involved and the difference in time and location.

There is a great difference in sensitivity, close to 35 dB, between the L-band radar at Millstone Hill and the Jicamarca radar, mainly due to the difference in antenna aperture and the possibility of coherent integration at 50 MHz. The longer the wavelength of the radar the longer the coherence time. It should be noted that the difference in sensitivity is not a consequence of a direct wavelength dependence since in the inertial subrange this dependence is in favor of shorter wavelengths, i.e., it is proportional to $\lambda^{-\frac{1}{3}}$; this can be derived from Eqs. (2) and (16).

As far as an explanation for the existence of strong echoes from mesospheric heights, we believe they are, again, due to neutral turbulence working in a medium with a gradient in index of refraction, with the difference that at these altitudes the index of refraction is determined by the existence of free electrons.

For the mesosphere the medium is not as well known as in the stratosphere. Different observation techniques give different values for the gradients in electron density. Also, the values we obtained for signal strength from any one particular height vary considerably in time; they range from the incoherent scatter level to 30 dB or more above this level (Rastogi and Woodman, 1974). Therefore, we shall only attempt here to show that reasonable values of electron density, electron density gradients, and length scales (L_0) give us signal enhancements in agreement with the observed values.

At these altitudes the electrons are strongly coupled to the neutrals and, within time scales smaller than the production and recombination times as well as molecular diffusion times for a 3 m structure, we can consider them as "passive additives" as defined by Tatarski (1961). In Appendix B we have derived the relationship

$$\frac{dn}{dz} = \frac{1}{2}\frac{d}{dz}(\ln N)\frac{f_p^2}{f^2}, \tag{26}$$

where dn/dz is the height derivative of the index of refraction in the ionosphere in terms of the logarithmic height derivative, $H = d(\ln N)/dz$, of electron density. Combining Eqs. (26), (16), (17) and (20) we get an expression for

$$P/P_i = \phi(k)/\phi_i(k) = 0.26(2\pi)^3 L_0^{\frac{4}{3}} k^{-11/3}(NL_0/H^2L), \tag{27}$$

where P/P_i is the enhancement ratio of "turbulent power" over the expected incoherent scatter power from the same altitude. If we take $N = 0.5\times10^9$ electrons m^{-3} as a typical value for 70 km (Prakash *et al.*, 1972), and $H = 10$ km and $L_0 = 100$ m as reasonable values for these parameters, we get $P/P_i = 196$, in good agreement with the observed values, and with the value shown in Fig. 2, in particular. Much steeper gradients of electron density have been observed at certain particular heights (Prakash, *et al.*). The coincidence of a turbulent level with regions having gradients with scale lengths of 1 km would produce radar echoes two orders in magnitude higher, explaining the higher echo powers that have been observed (Rastogi and Woodman, 1974) and first reported by Flock and Balsley (1967).

The spectrum width at mesospheric heights is smaller but comparable to the width observed at stratospheric heights, and could be explained in a similar manner with expected values of $\langle\Delta v^2\rangle^{\frac{1}{2}}$ produced by turbulence in a sheared region from one to a few hundred meters in thickness.

It is possible that the same mechanism responsible for the backscatter echoes at 50 MHz reported here is responsible for the echoes obtained from the D region in "partial-reflection" experiments (Gregory and Vincent, 1970). A joint experiment could help to establish with certainty if the echoes received using HF are partial reflections or backscattering from turbulent fluctuations of dielectric properties in the medium. It would also be of interest to establish the relationship between the scatter echoes we observe and the ionospheric forward scattering of VHF signals studied by Bailey *et al.* (1955) at high latitudes and used for communication purposes.

The gap between 35 and 55 km can be explained by the lack of free electrons below 55 km and of sufficient neutral density above 35 km.

b. *Wind velocity measurements*

We shall limit at this time our discussion of the wind measurements to stress the potential of the technique for the study of the dynamics of the neutral atmosphere at these altitudes. We will also mention some future improvements that are being developed which will increase the potential even further.

The most important feature of the wind measurements common to both altitude ranges, stratospheric and mesospheric, is the accuracy in the determination of the velocities and the time resolution. As has been mentioned before, typical accuracies are of the order of 2 and 20 cm sec^{-1} for the vertical velocities at stratospheric and mesospheric heights, respectively, and 20 cm sec^{-1} and 2 m sec^{-1} for the corresponding horizontal component. These accuracies combined with a time resolution of 1 min and with the continuity of the measurements permit the observation of the velocity field of waves from the shorter gravity wave periods to tidal and planetary waves, and certainly of the prevailing zonal and meridional winds and their long-term variations.

Our confidence in interpreting the short-period fluctuations in velocity as due to gravity wave oscillations has been ratified from the results of the spectral analysis of velocity time series as shown, for example, in Figs. 4 and 5. The frequency spectrum of these series show a consistent sharp cutoff at a period of 5–7 min consistent with the Brunt-Väisälä cutoff period predicted by theory (Hines, 1960); this analysis has been carried out and is reported by Rastogi and Woodman (1974). Further analysis is being performed and will be the subject of future publications.

Because of our present computer speed we are limited to observations at only one particular height at a given time. A data processing system with a third-generation computer is being implemented which will allow us to observe 20 heights simultaneously. This will permit us to observe the height structure of waves and their phase progression. We have also been limited to the observation of only two channels simultaneously which limits us to two velocity components. By splitting the antenna into two halves and into two separate polarizations each, we will be able to observe simultaneously in four different directions giving us the three orthogonal components of the velocity field with redundancy.

While the height resolution has been limited to 5 km by the present receiver bandwidth, the ultimate resolution will be limited by the transmitter bandwidth (minimum pulse length) to 2.5 km and hopefully to 1.5 km. This will permit us to resolve the separation of the different turbulent layers and their actual heights within a fraction of the pulse length.

7. Conclusions

The Jicamarca radar, or any lower VHF radar with comparable transmitter power and antenna size, can obtain information from backscatter echoes about the vector velocity field and turbulent processes in the atmosphere at altitudes between 10 to 35 km and 55 to 85 km. Velocities are obtained with sufficient accuracy, time resolution and continuity to allow us to study waves from the shortest gravity periods to tidal and planetary waves as well as the prevailing winds and their variation on annual scales. A mechanism based on neutral atmospheric turbulence produced by wind shear working on the height gradients of index of refraction has been proposed to explain the strength of the echoes received from these altitudes. The power strength as well as the spectrum width of the backscattered signals is consistent with this mechanism, if one assumes that turbulence is confined to layers of the order of 100 m in thickness.

The first three moments of the frequency spectrum of the radar echoes, which yield information about the power, Doppler shift and frequency width, can be obtained in terms of only two points of the correlation function. This technique is much simpler and faster than the conventional way of obtaining these parameters by a full evaluation of the frequency spectrum.

Acknowledgments. We would like to thank Gerardo Vera and the Jicamarca staff for their cooperation on this project.

We would like to acknowledge J. Green, T. Hagfors and C. G. Little, since we have benefited from their previous and unpublished power measurements in the 10–20 km region. They were the first to suspect that these "ground clutter" echoes were of stratospheric origin.

This work has been partially supported by the National Science Foundation and the Organization of American States.

APPENDIX A

Evaluation of Spectrum Moments from the Autocorrelation Function

We shall present here the derivation of the relationships used in the main text between the power, Doppler shift and the spectrum width, and the values of the correlation function at the origin and at a single small delay.

Taking the derivative with respect to time of the Fourier integral representing the function $C(\tau)$, we can obtain the well-known relationship between the derivatives at the origin and the moments of a transform pair, namely,

$$C(0)=\int F(\omega)d\omega=m_0, \tag{A1}$$

$$C'(0)=\int j\omega F(\omega)d\omega=jm_1, \tag{A2}$$

$$C''(0)=\int -\omega^2F(\omega)d\omega=-m_2. \tag{A3}$$

From the definitions of P, Ω and σ in terms of the moments m_0, m_1, m_2 [see Eqs. (7), (8) and (9)] we obtain

$$P=C(0), \tag{A4}$$

$$\Omega=\frac{jC'(0)}{C(0)}, \tag{A5}$$

$$\sigma^2=-\frac{C''(0)}{C(0)}+\frac{C'(0)}{C(0)}. \tag{A6}$$

We define the amplitude and phase of $C(\tau)$ by

$$C(\tau)\equiv A(\tau)e^{j\phi(\tau)}, \tag{A7}$$

where $A(\tau)$ and $\phi(\tau)$ are real and continuous functions of τ. If the moments of $F(\omega)$ exist, the derivatives of $C(\tau)$, $A(\tau)$ and $\phi(\tau)$ are well defined.

Since $C(\tau)$ is a complex autocorrelation, it has Hermitian symmetry, i.e., $C(\tau)=C^*(-\tau)$. It follows that $A(\tau)$ is an even function and $\phi(\tau)$ an odd function of τ. Using these properties and differentiating Eq. (A7), we have

$$C(0)=A(0), \tag{A8}$$

$$C'(0)=j\phi'(0)A(0), \tag{A9}$$

$$C''(0)=A''(0)-\phi'^2A(0). \tag{A10}$$

Combining (A4)–(A9), we have

$$\Omega=\phi'(0), \tag{A11}$$

$$\sigma^2=-\frac{A''(0)}{C(0)}, \tag{A12}$$

which are the identities used in the text.

For a sufficiently small τ we can approximate

$$\phi(\tau)\approx\phi'(0)\tau, \tag{A13}$$

with errors of order τ^3 and

$$A'(\tau)\approx A(0)+\tfrac{1}{2}A''(0)\tau^2, \tag{A14}$$

with errors of order τ^4.

If $C(\tau)$ is evaluated at a single, but sufficiently small delay, and at the origin, we can use (A13) and (A14) to estimate $\phi'(0)$ and $A''(0)$ to obtain Ω and σ as given by (A11) and (A12). The result is

$$\Omega=\frac{\phi(\tau_1)}{\tau_1}, \tag{A15}$$

$$\sigma^2=\frac{2[1-A(\tau_1)/C(0)]}{\tau_1^2}. \tag{A16}$$

It is interesting to note that (A15) becomes an identity for any value of τ if the spectrum $F(\omega)$ is symmetric with respect to the frequency shift Ω. In this case using the displacement theorem for Fourier transforms, one can show that

$$C(\tau)=A(\tau)\exp(j\Omega\tau). \tag{A17}$$

The approximation (A13) becomes an identity for any value of τ, as does (A15) as well.

APPENDIX B

On the Spatial Spectrum of Fluctuations in a Plasma

We shall derive two expressions, one for the three-dimensional spatial spectrum of the fluctuations in index of refraction for a plasma in thermodynamic equilibrium, and the other for the height derivative of index of refraction of a plasma in terms of the plasma frequency and a scale height.

Most of the theories about fluctuations in plasmas treat the fluctuations in either the electric field or the electron density. We need an expression for the fluctuations in index of refraction.

The index of refraction in a plasma for a wave of frequency $f\gg f_p$ is given by

$$n=1-\tfrac{1}{2}\frac{f_p^2}{f^2}, \tag{B1}$$

where f_p is the plasma frequency of the medium and is proportional to N, the electron density. We write, explicity,

$$f_p^2=KN. \tag{B2}$$

A differential in n, Δn, is given by

$$\Delta n=\frac{f_p^2\Delta N}{2f^2N}. \tag{B3}$$

We can then write the spatial correlation of $\Delta n(x)$, in terms of the spatial correlation for $\Delta N(x)$:

$$\langle \Delta n(\mathbf{x})\Delta n(\mathbf{x}+\mathbf{r})\rangle = \frac{f_p^4}{4f^4N^2}\langle \Delta N(\mathbf{x})\Delta N(\mathbf{x}+\mathbf{r})\rangle. \quad \text{(B4)}$$

In terms of their respective Fourier transforms, we have

$$\phi(k) = \frac{f_p^4}{4f^4N^2}\phi_N(k). \quad \text{(B5)}$$

For a plasma in thermodynamic equilibrium and for wavelengths, which in our case, are much larger than the Debye length, it is found that (see, e.g., Salpeter, 1963)

$$\phi_N(\mathbf{k}) = \frac{N}{2(2\pi)^3}. \quad \text{(B6)}$$

[The $(2\pi)^3$ term is not in the reference and comes from our definition for a Fourier transform]; using this expression $\phi(k)$becomes

$$\phi(k) = \frac{f_p^4}{16\pi^3 N f^4}. \quad \text{(B7)}$$

Differentiating (A1), we can also find an expression for dn/dz, namely,

$$\frac{dn}{dz} = -\frac{1}{2}\frac{d}{dz}(\ln N)\frac{f_p^2}{f^2}. \quad \text{(B8)}$$

Expressions (B6) and (B7) have been used in the main text.

REFERENCES

Bailey, D. D., R. Bateman and R. C. Kirby, 1955: Radio transmission at VHF by scattering and other processes in the lower ionosphere. *Proc. IRE*, 43, 1881–1230.

Balsley, B. B., 1969: Some characteristics of non-two-stream irregularities in the equatorial electrojet. *J. Geophys. Res.*, **74**, 2333–2347.

Barbé, G. D., 1971: Structure de la stratosphère mayenne et elevees. Detection de la turbulence en ciel clair. Application aux vola envisages pour les avions de transport supersoniques. Paper presented at the Joint Conf. on Aeronautical Meteorology, Paris, 24–26 May [Some of the results of interest are shown by Reiter (1972)].

Booker, H. G., and W. E. Gordon, 1957: The role of stratospheric scattering in radio communication. *Proc. IRE*, **45**, 1223–1227.

Cadet, D., 1973: Étude du gradient vertical de vent horizontal dans la stratosphere. Thèse de Docteur, Université de Paris.

Crane, R. K., 1970: Measurement of clear air turbulence in the lower stratosphere using the Millstone Hill L-band radar. *Preprints 14th Radar Meteor. Conf.*, Tuscon, Ariz., Amer. Meteor. Soc., 101–106.

Evans, J. V., 1969: Theory and practice of ionosphere study by Thomson scatter radar. *Proc. IEEE*, **57**, 496–530.

Farley, D. T., Jr., 1963: Two-stream plasma instability as a source of irregularities in the ionosphere. *Phys. Rev. Letters*, **10**, 279–282.

Flock, W. L., and B. B. Balsley, 1967: VHF radar returns from the D region of the equatorial ionosphere. *J. Geophys. Res.*, **72**, 5537–5541.

Gregory, J. B., and R. A. Vincent, 1970: Structure of partially reflecting regions in the lower ionosphere. *J. Geophys. Res.*, **75**, 6387–6389.

Hardy, K. R., 1972: Studies of the clear atmosphere using high power radar. *Remote Sensing of the Troposphere*, V. E. Derr, Ed., Boulder, Colo., NOAA and the University of Colorado, 14-1 to 14-33 (Govt. Printing Office).

Hines, C. O., 1960: Internal gravity waves at ionospheric heights. *Can. J. Phys.*, 38, 1441–1481.

Lindzen, R. S., and S. Chapman, 1969: Atmospheric tides. *Space Sci. Rev.*, **10**, 2–188.

Prakash, S., B. H. Subbaraya and S. P. Gupta, 1972: Electron density profiles in the equatorial lower ionosphere at Thumba. *COSPAR Symposium on D- and E-Region Ion Chemistry—An Informal Symposium Record*, C. F. Sechrist Jr. and M. A. Geller, Eds., University of Illinois, Aeronomy Rept. No. 48, 359–363.

Rastogi, P. K., and R. F. Woodman, 1974: Mesospheric studies using the Jicamarca incoherent scatter radar. *J. Atmos. Terr. Phys.* (in press).

Reiter, R., 1972: Fundamental problems of atmospheric science. *Remote Sensing of the Troposphere*, V. E. Derr, Ed., Boulder, Colo., NOAA and the University of Colorado, 2-1 to 2-28 (Govt. Printing Office).

Salpeter, E. E., 1963: Density fluctuations in a nonequilibrium plasma. *J. Geophys. Res.*, **68**, 1321–1333.

Tatarski, V. I., 1961: *Wave Propagation in a Turbulent Medium.* New York, McGraw-Hill, 285 pp.

Tennekes, H., and J. L. Lumley, 1972: *A First Course in Turbulence.* The M. I. T. Press, 300 pp.

Wilson, D. A., and L. J. Miller, 1972: Atmospheric motion by Doppler radar. *Remote Sensing of the Troposphere*, V. E. Derr, Ed., Boulder, Colo., NOAA and University of Colorado, 13-1 to 13-34 (Govt. Printing Office).

Woodman, R. F., and T. Hagfors, 1969: Methods for the measurement of vertical ionospheric motions near the magnetic equator by incoherent scattering. *J. Geophys. Res.*, **74**, 1205–1212.